REPORT

The effect of lunar declination on CO_2 degassing from central Italian Apennines

Pierpaolo Zuddas[1,*] and Fernando Lopes[2]

*Correspondence: pierpaolo.zuddas@sorbonne-universite.fr

Received: January 11, 2024; Accepted: May 6, 2024; Published Online: May 15, 2024; https://doi.org/10.59717/j.xinn-geo.2024.100073

GRAPHICAL ABSTRACT

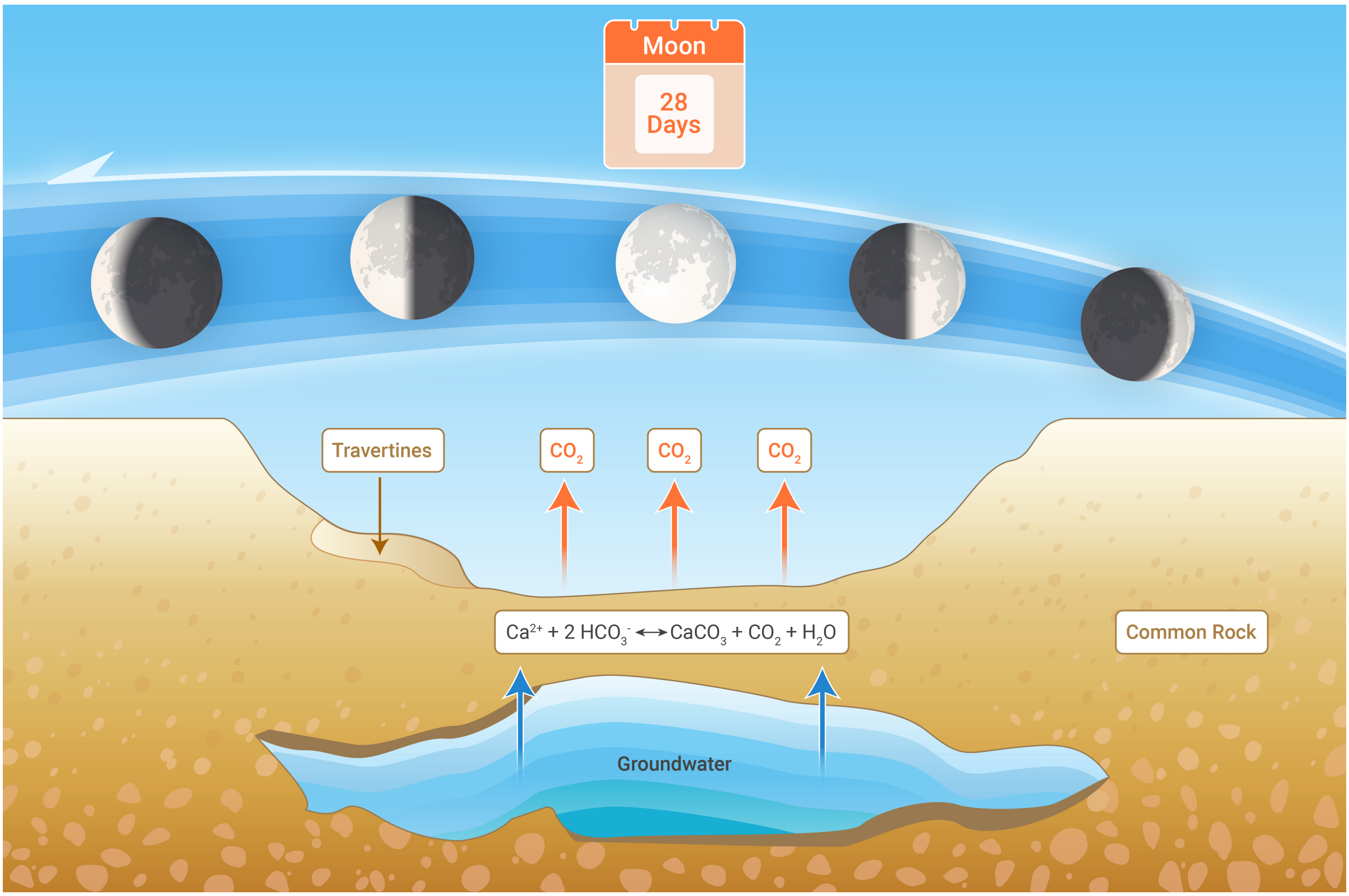

PUBLIC SUMMARY

- The variation of aquifer's chemical composition is related on periodical lunar tides in central Italian Apennines.
- Lunar tides trigger fluid movement leading to periodic CO_2 degassing from over-pressured reservoirs.

The effect of lunar declination on CO_2 degassing from central Italian Apennines

Pierpaolo Zuddas[1,*] and Fernando Lopes[2]
[1]Sorbonne Université, Paris 75005, France
[2]Muséum National d'Histoire Naturelle, Paris 75005, France
*Correspondence: pierpaolo.zuddas@sorbonne-universite.fr
Received: January 11, 2024; Accepted: May 6, 2024; Published Online: May 15, 2024; https://doi.org/10.59717/j.xinn-geo.2024.100073

Citation: Zuddas P. and Lopes F. (2024). The effect of lunar declination on CO_2 degassing from central Italian Apennines. The Innovation Geoscience 2(2): 100073.

The periodical degassing from CO_2 over-pressured reservoirs may have serious consequences for the environment making urgent understanding the processes and forecasting the frequency. Prediction though needs methods that depends from temporal and spatial properties of hydro-chemical and physical reservoir characteristics that unfortunately are often lacking. We have analyzed surface emissions of CO_2 attributed to over-pressured CO_2-rich reservoirs in the Central Italian Apennines a zone characterized by significant periodical CO_2 degassing. Here aquifers are hosted in Mesozoic limestone with high pCO_2 groundwater and travertine deposits. We analyzed a 10-year temporal series and found that in the Apennines CO_2 flux and aquifer fluid composition are correlated with the lunar tides. In particular, our study reveals that low CO_2 flux corresponds with low lunar tidal potential values. We found a similar trend for dissolved calcium and water alkalinity, while pH values display a linear correlation with tidal cycles. The forces associated with tidal potentials are not capable of fracturing rock. However, they can, under certain conditions, drive the flow of fluids in over-pressured reservoirs, triggering sub-surface fluid movements that in turn modify the water–rock reactivity. In the central Apennines, we show that these movements result in increased dolomite dissolution and an eventual return to calcite equilibrium. In this case, dolomite dissolution breaks the rock releasing calcium into ground water, which leads to calcite equilibrium and in turn to the formation of significant quantities of travertine and the concomitant release of CO_2 in the atmosphere.

INTRODUCTION

The response of aquifers to earth and lunar tide strains has long been observed and recognized in several situations for more than one century[1,2] and recently used to provide specific estimation storage and permeability of the aquifers.[3] The potential impact of these strains has also been proposed as responsible for changes in stress and pore pressure in porous and in water-saturated formations.[4] However, despite lunar tides are ubiquitous on the earth, the potential impacts of tides have never been evaluated in over pressured reservoirs. These reservoirs may occur naturally in particular geological situations or in low carbon strategies such as the geological sequestration of CO_2 or in the more traditional CO_2-enhanced recovering when CO_2 is injected into oil field to increase energy production.[5] The distribution of CO_2 emission, in the Central Italian Apennines corresponds the formation of reservoirs fed by fluids rising through processes that imply the production and accumulation of CO_2 in the Earth's upper crust.[6,7] Similarly, the geological CO_2 storage, a critical technology for environmental energy, produce oversaturated fluids conditions that may generated a CO_2 plume in the subsurface.[8] The mechanisms that determine this process have complex and nonlinear interactions with geological properties (permeability, depth, thickness) and have been tentatively explained by the interaction between CO_2-saturated and CO_2-oversaturated aquifers.[9,10] It is today difficult to predict the frequency of CO_2 variations using hydrogeological models because aquifer models assume that conditions are 'perfectly confined' or 'purely unconfined', whereas boundary conditions vary for regional-scale aquifers.[3,11-14] Real temporal chemical measurements directly reflect these variations[15] as they take into account possible low tectonic stress and periodical lunar tide oscillations that locally reshape the aquifers.[11,16-24]

In our study, we have used the chemical composition records on springs and well in the Central Apennine area (Central Italy) collected over a 10-year period (2009-2018).[10] We have calculated the CO_2 emissions in this area confirming earlier estimates that indicate that the quantity of CO_2 released into the atmosphere from 2009-2018 in this zone is equivalent to the total amount of CO_2 released by Mount Etna (Italy), the Earth's premier CO_2-producing volcano over the same period. This amount is by over 1800 kt of $CO_{2,}$ equivalent to a CO_2 flux of 10^{11} mol yr^{-1} that should correspond to 10% of the overll Earth flux for this range of time.[18,25] In this paper we report a relation between lunar tides and the observed variation of CO_2 degassing during 10 years of monitoring in a non-volcanic area. We show for the first time the influence of lunar tides on water-rock reactivity and offer a geochemical mechanism explaining the observed variability of CO_2 degassing from the natural aquifers of central Apennines.

MATERIALS AND METHODS

The Italian Apennine region is home to several aquifers hosted in Mesozoic limestone and has frequent and significant gas emissions and numerous soda springs and wells with high pCO_2 groundwater and travertine deposits at the surface. Crustal thickness in the central Apennines is approximately 35 km, heat flow is normal and gravity anomalies are negative. The current tectonic deformation field is characterized by an extension in the axial zone of the Apennine chain and by a contraction responsible for periodic earthquakes of moderate magnitude (between 4 and 6), originating mainly in the upper crust.[26] They are generated by active lithospheric thrusts beneath the Apennine watershed and are generally associated with low-angle normal faults accommodating uplift of basement culminations. The large amount of CO_2 released into the atmosphere is most probably controlled by diffusive processes and the regional hydrogeological features of the degassing area (Figure 1). The zone under scrutiny covers 700 km^2 and is also characterized by numerous natural springs and wells that release CO_2 oversaturated water at the rate of hundreds of liters per second. The water releases CO_2 into the atmosphere and produces large travertine deposits that have been quarried since ancient roman times, over 2000 years ago. Field data used in this study (major and minor chemical fluid composition and dissolved CO_2) was collected from the 36 main springs and wells of the two large reservoirs, sampled between April 2009 and December 2018.[10]

We have recalculated pCO_2 partial pressure using field alkalinity and pH data and the overall water composition, using the PHREEQC software and thermodynamic database.[27] Springs, gas vents and travertine are potentially controlled by regional hydrology and meteoric water. The hydrological recharge is located in the Mesozoic limestone layers that overlay a thick and relatively impermeable cover of Oligocene–Neogene clastic sediments. Spring distribution is dictated by water circulation in the Mesozoic limestone, where water chemical composition is between Ca–SO_4 and Ca(Mg)–HCO_3, with very limited amounts of Na–HCO_3, Na–Cl and Na–SO_4.

To estimate the Lunar tides, we have considered that the Earth is spherically symmetrical, nonrotating and has self-gravity with elastic and isotropic properties in an initial equilibrium state. The Moon and the Sun are considered celestial bodies that produce a tidal effect on the Earth. Assuming M = Earth masse and m = Moon masse, every point P at the Earth's surface is subject to a force γ equal to:

$$\gamma = GMm\boldsymbol{PA'}(PA')^3 \qquad (1)$$

Where $\boldsymbol{PA'}(PA')^3$ is the vector distance between the point P at the Earth's surface and the Moon's center of gravity A', while G is the gravitational constant of Newton. The Earth is subject to an attraction force, $\boldsymbol{\gamma_E}$, from the Moon equal to:

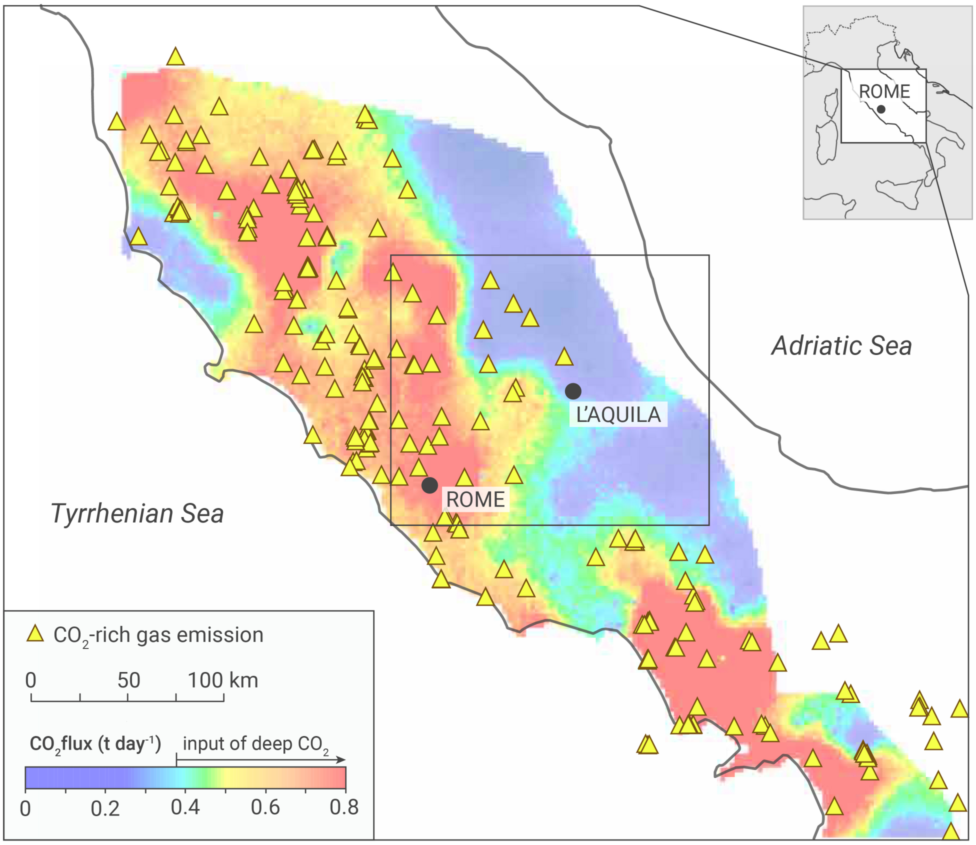

Figure 1. Map of CO_2 degassing and location of the investigated aquifers (from Chiodini et al. 2020).

$$\gamma_E = \frac{GmAA'}{(AA')^3} \quad (2)$$

Where A is the Earth's center of gravity, ***AA'***$(AA')^3$ is the vector distance between the Earth's center of gravity and the Moon's center of gravity. The difference between the Moon's attraction on *P* and the Earth's attraction on the Moon, also called Earth tide force, ***f***, is the difference between $\boldsymbol{\gamma}$ and $\boldsymbol{\gamma_E}$. The gravitational force **f** can be expressed as a function of its potential **w**:

$$w = Gm\left[\frac{1}{PA'} - \frac{-APxAA'}{(AA')^3}\right] \quad (3)$$

Since the position of point *P* on the Earth's surface is a function of the latitude *z*, we have expressed the Earth's tide potential ***w*** using Legendre polynomials:

$$w = \frac{Gm}{D} x \sum_{n=0}^{\infty} \left(\frac{R}{D}\right)^n xPn(\cos z) \quad (4)$$

Where *D* is the distance between the Earth's center of gravity and the Moon's center of gravity, *R* is the distance between the given point *P* and the Earth's center of gravity and P^n, is the Legendre polynomial function. The Earth's tidal potential ***w*** can be approximated to the second order Legendre polynomial term:

$$w_2 = \frac{GmR^2(3\cos^2 z - 1)}{2D^3} \quad (5)$$

Using lunar ephemeris and effective latitude positions were provided by the *Institut de Mécanique Céleste et de Calcul des Éphémérides* (IMCCE). We have calculated the attraction force generated by the Moon on the Earth (*w*), also called lunar tidal potential or tidal oscillations, using an average latitude of 43°.[28]

RESULTS

The principal lunar tide oscillations estimated by our mechanical calculations show a periodicity of 27.555 days. This value of periodicity results from the variation in the distance between the Earth and the Moon in the central Apennines. The lunar tidal potential responsible for the attraction force on the Earth calculated by Eqn. 5 is reported in Figure 2. The lunar tidal signal (potential) is a continuous function due to the lunar attraction while data points concerning the pCO_2 partial pressure are independent on the lunar signal and should be randomly distributed along the continuous curve. We found that different pCO2 partial pressure are systematically (95% of points) found at extrema of the lunar potential indicating that the is a very strong (at least 95%) correlation (the tidal signal being complex sinusoid) between concentration variations and the w_2 attraction. We were surprised by the existence of such a strong correspondence correlation, given that there is no clear mechanistic relationship between pCO_2 partial pressure and tidal potentials.

We have focused our attention on the data set gathered from June 2009-June 2010 because it was the largest and densest of the 10-year period. Figure 3A illustrates those variations in different

calcium concentrations are systematically (95% of values) found at extrema of the lunar potential. Given that calcium concentrations are not distributed along the continuous curve, it is not possible to identify a continuous function between tidal potential variations and calcium concentrations using one-year data set. We can safely say however, based on our data sets, that minimum calcium concentrations are indeed related to weak Lunar tide potentials while higher calcium values are related to high Lunar potential values.

Figure 3B shows that variations in alkalinity concentration are concentrations are systematically (95% of points) at extrema of the lunar potential and not y distributed along the continuous curve. Similar to calcium, the lack of intermediate concentration values makes not possible identifying a continuous function for alkalinity. Figure 3C shows that variation of pCO_2 partial pressure that range between 0.01 atm. and 1.7 atm. is systematically found at the extrema of the lunar potential. Low pCO_2, (from 0.01 to 0.2 atm) corresponds to a weak Lunar potential while higher pCO_2 values (from 1.4 to 1.6 atm) correspond to stronger Lunar potential. These observations suggest that CO_2 emissions in the zone may be related to Lunar tidal forces in a discontinuous and apparently non-linear relationship.

We considered that is possible that pCO_2 variations may reflect changes in chemical reactivity in the aquifer and if that is indeed the case, it should be reflected in fluid pH variations. In fact, variations in fluid pH globally reflect the complex process of water-rock interaction because pH participates in both carbonate and silicate mineral dissolution and precipitation reactions. Figure 4 illustrates that pH significantly varies between a minimum of 6.2 and a maximum of 8.2. However, unlike calcium, alkalinity and pCO_2 partial pressure, pH values are distributed along the lunar potential curve during the 27.55-day period indicates the presence of possible water-rock interaction processes responsible for the observed release of CO_2.

To explain the different behavior of pH, we have estimated the mineral saturation indexes (SI) of the water and found that sampled fluids are close to equilibrium with respect to calcite given that $SI_{calcite}$ is between -0.7 and +0.3 with mean value of -0.1. It is likely that the principal process that controls groundwater composition is calcite dissolution in near-equilibrium conditions.[18] The collected ground waters are under-saturated with respect to gypsum or anhydrite ($CaSO_4$, $2H_2O$, $CaSO_4$ respectively) although it is possible that gypsum or anhydrite dissolution does take place in springs with high SO_4 content. When gypsum or anhydrite dissolves, it can facilitate dolomite dissolution because of the common ion effect.[29] This in turn could allow for

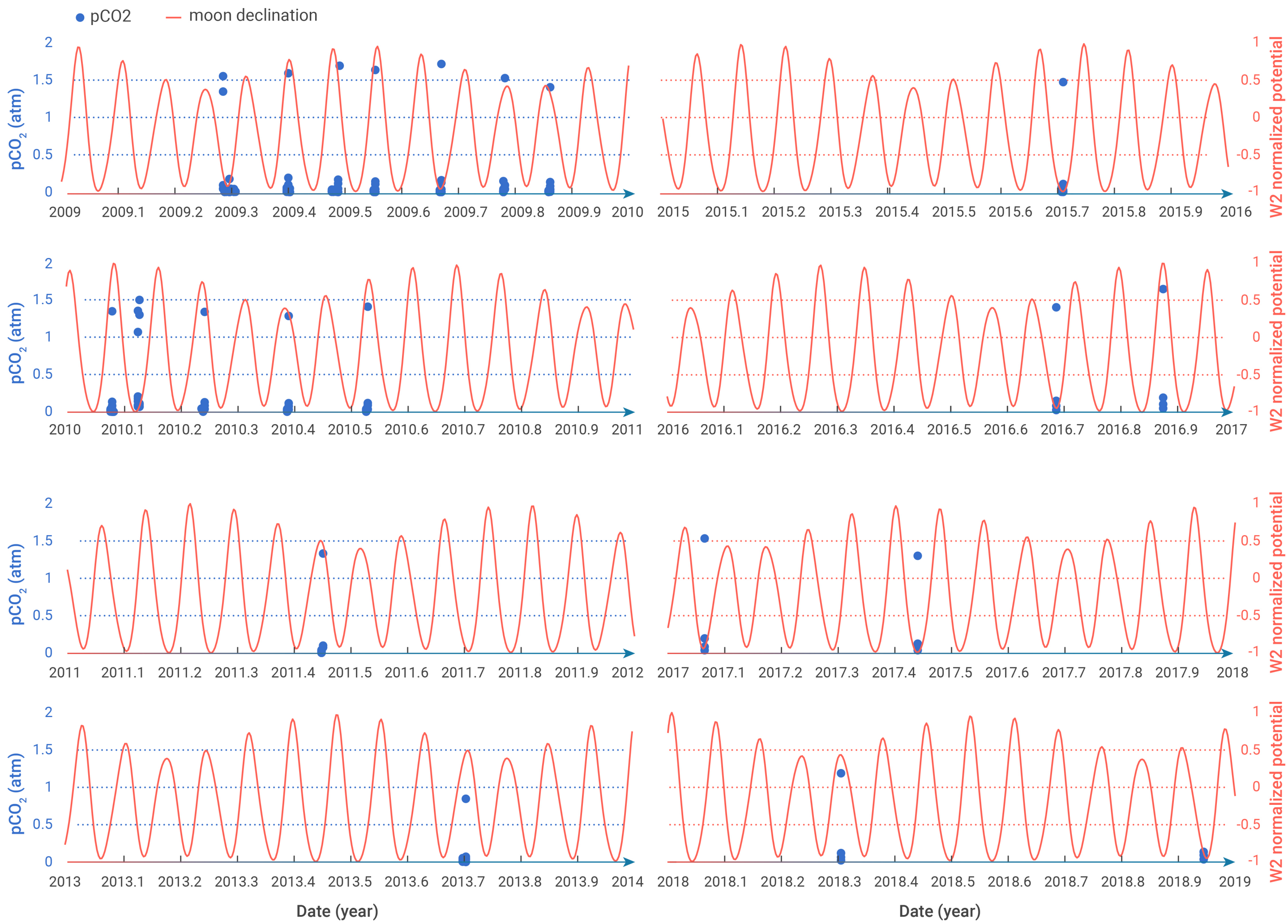

Figure 2. Evolution of pCO_2 partial pressure and Lunar tide potential estimated by Eqn.5 during the 10 years of investigation.

increased calcite precipitation maintaining calcite in near-equilibrium conditions. Additional processes such as halite dissolution from evaporate formation may effect groundwater composition in the studied zone, given that clay-water equilibria may contribute to the observed continuous pH variations.

However, tidal forces are too weak to fracture rock compared to tectonic forces.[30] We have estimated the vertical force acting on a unit mass at the average latitude for the investigated zone and found that the average force is close to 5.6 x 10^{-7} N Kg^{-1}. Given the pressure gradient associated with tidal potential, the pressure between the surface and the first 10-15 Km (i.e. the transition between ductile and brittle crust) is approximately 10 Pa for an average rock density of 2.4 Kg m^3. This value is lower by several orders of magnitude than the 0.1-0.20 MPa required to fracture carbonate rock in tensile stress.[31] 10 Pa of tidal pressure may however drive fluid flow in stressed localized areas, increasing the movement of subsurface fluids.[4] Groundwater at different depths may therefore be affected by tidal forces[32] and carry with it the gas accumulated in buried highly pressurized aquifers as it travels towards the surface. At the fault planes, fluid pressure is reduced and local aquifers may connect favoring CO_2 release[33] with consequent carbonate precipitation, in agreement with the following the classical reaction path:

$$Ca^{2+} + 2HCO_3^- \rightarrow CaCO_3 + H_2O + CO_2 \uparrow \quad (6)$$

The formation of calcium carbonate deposits evidenced by the large quantities of travertine in the zone and the significant release of CO_2 point to disequilibrium conditions generated by a reduction in CO_2 pressure.[18,34] When tidal potential is high and the Moon is close, aquifer depths are highest and fluids are oversaturated with respect to calcite; whereas when tide potential is low, fluids are close equilibrium with calcite. Although lunar tides exert only weak stress on rock[35] without fracturing it,[31] they do indeed produce weak vertical fluid movements[18,34] causing ex-solution from CO_2-rich waters. This process, similar to the mechanical bubbling that occurs when you shake a bottle of carbonated soda, modifies the system's overall chemical equilibrium[36] and generates fluid releasing processes. The observed variations in central Apennine CO_2 release may correspond to gas separation and the ascent of CO_2 through fluid movements triggered by the lunar declination.

As confirmed by our investigation, tides are harmonic functions characterized by amplitudes and phases that simultaneously act as stressors on the subsurface, the contribution of lunar tides on the groundwater response can now be disentangle. We propose that systematically exploring the influence of subsurface properties on the tidal transfer function, the relationship between the amplitude and the phase of the stressors and the resulting chemical transport reactivity responsible for CO_2 releasing could be potentially predicted.

CONCLUSIONS

Our observational scale work shows the relation between lunar tides and CO_2 releasing in over-pressured CO_2 aquifers. The pressurized carbonate fluids rise to the surface through pre-existing faults producing variable amounts of CO_2 that are potentially released into the atmosphere. We propose that carbonate mineral dissolution under calcite near-equilibrium conditions may be responsible for the observed CO_2 variations in the Central Apennines and that changes in fluid dynamics can be triggered by periodical tidal potential variations.

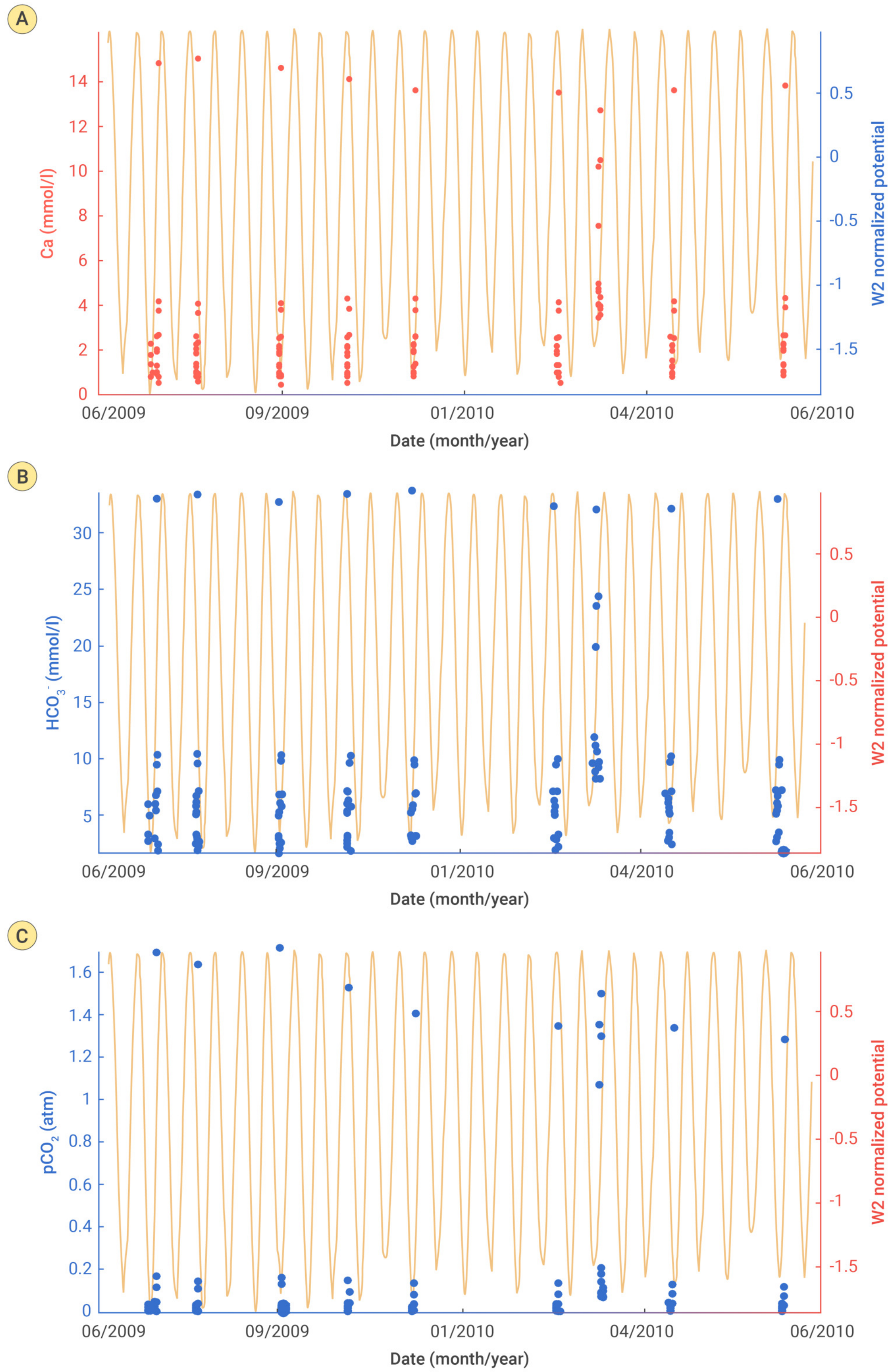

Figure 3. Evolution of calcium, HCO_3^-, and pCO_2 over time (A) Evolution of calcium concentration (red dots) as a function of time for the year: June 2009-June 2010. The continuous black line corresponds to the continuous W potentials estimated by Eqn. 5. (B) Evolution of HCO_3^- (alkalinity) (blue dots) as a function of time for the year: June 2009-June 2010. The continuous black line corresponds to the continuous W potentials estimated by Eqn.5. (C) Evolution of pCO_2 partial pressure (blue dots) as a function of time for the year: June 2009-June 2010. The continuous black line corresponds to the continuous W potentials estimated by Eqn. 5.

The analysis of long-term time series of CO_2 discharge and chemical fluid composition variations show that periodical low values of CO_2 released are correlated to the minimum lunar periodical tides of the zone. The combination of tidal potentials with traditional reactive transport description constraining poro-elastic and hydraulic parameter space can be potentially integrated in future predictive modelling of the CO_2 releasing from natural and artificial over pressured CO_2 reservoirs.

REFERENCES

1. Klomme, F. (1880). Die periodischen Schwankungen des Wasserspiegels in den inundierten Kohlenschachten von Dux in der Periode. Wien, Mathematisch-Naturwlssenschaftllchen Classe 8(1): 1−5.
2. Meizer, O.E. (1928). Compressibility and elasticity of artesian aquifers. Economic Geology 23(3): 263−291.
3. Allègre, V., Brodsky, E. E., Xue, L.,et al. (2016). Using earth-tide induced water pressure changes to measure in situ permeability: A comparison with long-term pumping tests. Water Resources Research 52(4): 3113−3126. DOI: 10.1002/2015WR017346.

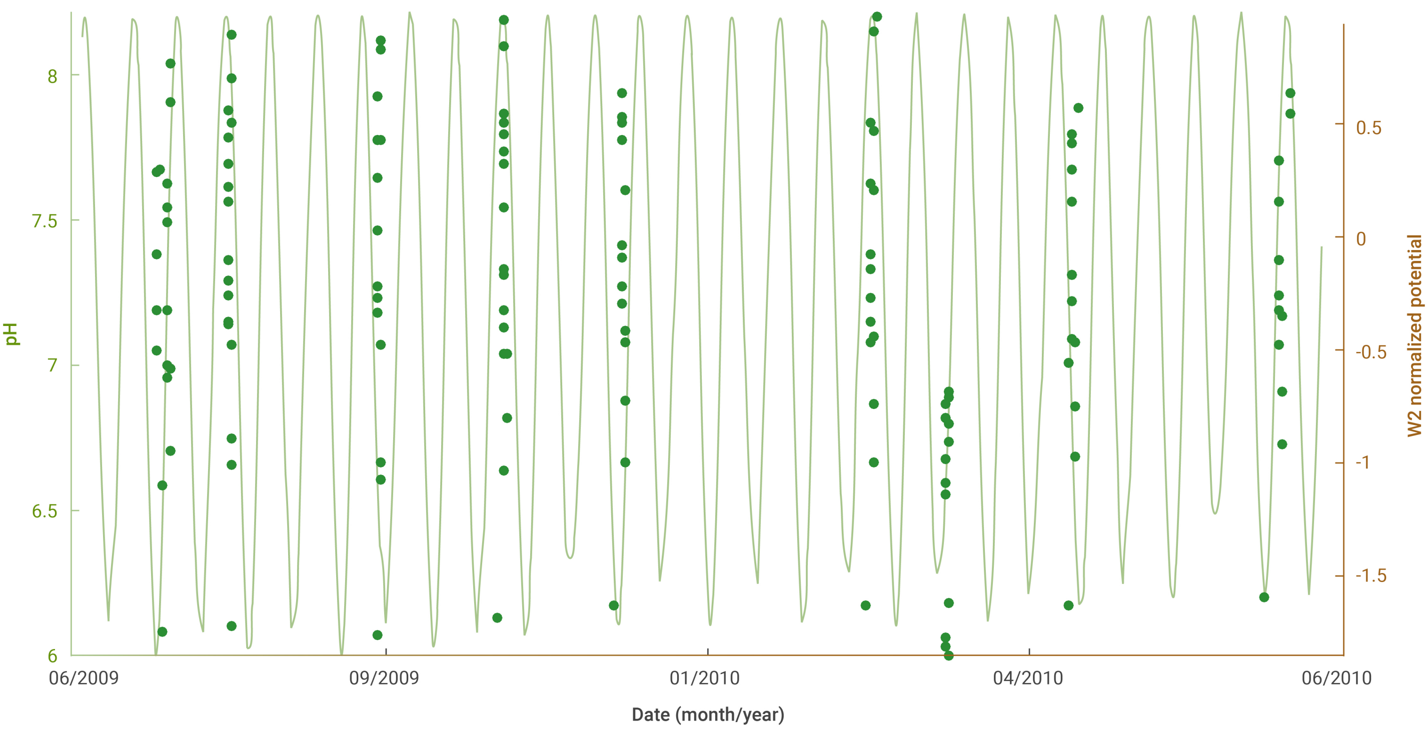

Figure 4. Evolution of pH (green dots) as function of time for the year: June 2009-June 2010 The continuous black line corresponds to the continuous W potentials estimated by Eqn.5.

4. McMillan, T.C, Rau, G.C., Timms, W.A, et al. (2019). Utilizing the impact of earth and atmospheric tides on groundwater systems: A review reveals the future potential. Rev in Geophysics 57(2): 281-315. DOI: 10.1029/2018RG000630.
5. Lake, L.W. and Lotfollahi, Bryant S.L.(2019). CO_2 enhanced oil recovery experience and its messages for CO_2 storage. In Science of Carbon storage in deep saline formations, Elsevier: 15-31. DOI: 10.1016/B978-0-12-812752-0.00002-2.
6. Uysal, I. T., Feng, Y. X., Zhao, J. X. et al. (2009). Hydrothermal CO_2 degassing in seismically active zones during the late Quaternary. Chemical Geology 265(3-4): 442–454. DOI: 10.1016/j.chemgeo.2009.05.011.
7. Tamburello, G., Pondrelli, S., Chiodini, G., et al, (2018). Global-scale control of extensional tectonics on CO_2 earth degassing. Nature Communications 9(1): 1-9. DOI: 10.1038/s41467-018-07087-z.
8. Middleton, R.S., Ogland-Hand, J.D., Chen B. et al. (2020). Identifying geological characteristics and operational decisions to meet global carbon sequestration goals. Energy & Environmental Science 13(12): 5000–5016. DOI: 10.1039/d0ee02488k.
9. Giammarco S., Palano M., Scaltrito A., et al. (2008). Possible role of fluid overpressure in the generation of earthquake swarms in active tectonic areas: The case of the Peloritani Mts. (Sicily, Italy). Journal of Volcanology and Geothermal Research: 178(4): 795–806. DOI: 10.1016/j.jvolgeores.2008.09.005.
10. Chiodini, G., Cardellini, C., Di Luccio, F.,et al. (2020). Correlation between tectonic CO_2 Earth degassing and seismicity is revealed by a 10-year record in the Apennines, Italy. Science Advances 6(35): eabc2938. DOI: 10.1126/sciadv.abc2938.
11. Hsieh, P. A., Bredehoeft, J. D., and Farr, J. M. (1987). Determination of aquifer transmissivity from Earth tide analysis. Water Resources Research, 23(10): 1824-1832. DOI: 10.1029/WR023i010p01824.
12. Galloway, D. L. and Rojstaczer, S. A., (1988). Inferences about formation elastic and fluid flow properties from the frequency response of water levels to atmospheric loads and earth tides: 4th Canadian/American conference on hydrogeology: Fluid flow", Heat Transfer and Mass Transport in Fractured Rocks, Banff, Alberta, Canada, June, 21-24:100–113.
13. Roeloffs, E., (1996). Poroelastic techniques in the study of earthquake-related hydrologic phenomena. Advances in Geophysics, 37: 135-195. DOI: 10.1016/S0065-2687(08)60270-8.
14. Christenson, S., Osborn, N. I., Neel, C. R., et al. (2011). Hydrogeology and simulation of groundwater flow in the Arbuckle-Simpson aquifer, south-central Oklahoma, U. S. Geological Survey. https://pubs.usgs.gov/sir/2011/5029/SIR2011-5029.pdf.
15. Wang, C. Y., Doan, M. L. et al. (2018). Tidal response of groundwater in a leaky aquifer—Application to Oklahoma. Water Resources Research 54(10): 8019–8033. DOI: 10.1029/2018WR022793.
16. Craig, T.J., Chanard, K., and Calais, E. (2017). Hydrologically-driven crustal stresses and seismicity in the New Madrid Seismic Zone. Nature Communications 8: 2143. DOI: 10.1038/s41467-017-01696-w.
17. Rogie, J. D., Kerrick, D. M., et al. (2000). Flux measurements of nonvolcanic CO_2 emission from some vents in central Italy. Journal of Geophysical Research: Solid Earth 105(B4): 8435-8445. DOI: 10.1029/1999JB900430.
18. Chiodini, G., Granieri, D., et al. (2010). Non - volcanic CO_2 Earth degassing: Case of Mefite d'Ansanto (southern Apennines), Italy. Geophysical Research Letters 37: L11303. DOI: https://doi.org/10.1029/2010GL042858.
19. Merritt, M. L. (2004). Estimating hydraulic properties of the Floridan aquifer system by analysis of earth-tide, ocean-tide, and barometric effects, *Collier and Hendry Counties, Florida"*, No. 3. US Department of the Interior, US Geological Survey. https://pubs.usgs.gov/wri/wri034267/wri03_4267.pdf.
20. Robinson, Edwin S., and R. Thomas Bell. (1971). Tides in confined well - aquifer systems. Journal of Geophysical Research 76(8): 1857-1869. DOI: 10.1029/JB076i008p01857.
21. Dean, G. A., Hardy, R., and Eltvik, P. (1994). Monitoring compaction and compressibility changes in offshore chalk reservoirs", SPE Formation Evaluation, 9(01): 73-76. DOI:10.2118/23142-PA.
22. Morland, L. W., and E. C. Donaldson (1984). Correlation of porosity and permeability of reservoirs with well oscillations induced by earth tides. Geophysical Journal International 79(3): 705-725. DOI: 10.1111/j.1365-246X.1984.tb02864.x.
23. Bredehoeft, J. D. (1967). Response of well - aquifer systems to Earth tides. Journal of Geophysical Research 72(12): 3075–3087. DOI: 10.1029/JZ072i012p03075.
24. Jacob, C. E. (1940). On the flow of water in an elastic artesian aquifer. Eos, Transactions American Geophysical Union 21(2): 574–586. DOI: 10.1029/TR021i002p00574.
25. Allard, P., Carbonnelle, J., Dajlevic, D., et al. (1991). Eruptive and diffuse emissions of CO_2 from Mount Etna. Nature 351(6325): 387–391. DOI: 10.1038/351387a0.
26. Bonfanti P. Genzano N., Heinicke, et al. (2012). Evidence of CO_2-gas emission variations in the Central Apennines (Italy) during the L'Aquila seismic sequence (March-April 2009). Bollettino di Geofisica Teorica ed Applicata 53(1): 147–168. DOI: 10.4430/bgta0043.
27. Parkhurst, D.L., Appelo, C.A.J., et al., (2013). Description of input and examples for PHREEQC version 3 - a computer program for speciation, batch-reaction, one-dimensional transport, and inverse geochemical calculations. U.S. Geological Survey Techniques and Methods. 6(A43): 497. DOI: 10.1016/0029-6554(94)90020-5.
28. Morse J.W. and Mackenzie F.T. (1990). Geochemistry of sedimentary carbonates. Developments in Sedimentology 48: 707p.
29. Stewart, R. H. (2007). Introduction to Physical Oceanography. Texas A&M University. 345pp. https://hdl.handle.net/1969.1/160216.
30. Mauk F.J. and Johnston M.J.S. (1973). On the triggering of volcanic eruptions by Earth tides. Journal of Geophysical Research 78(17): 3356. DOI: 10.1029/JB078i017p03356.
31. Schultz, R.A. (1996). Relative scale and the strength and deformability of rock masses. Journal of Structural Geology 18(9): 1139–1149. DOI: 10.1016/0191-8141(96)00045-4.
32. Stillings, M., Lunn, R. J., Pytharouli, S., et al. (2020). Microseismic events cause significant pH drops in groundwater. Geophysical Research Letters 48(2):

e2020GL089885. DOI: 10.1029/2020GL089885.
33. Frondini F., Cardellini C., et al. (2019). Measuring and interpreting CO_2 fluxes at regional scale: The case of Apennines, Italy. Journal of the Geological Society 176(2): 408-416. 10.1144/jgs2017-169.
34. Girault, F., Adhikari, L. B., et al. (2018). Persistent CO_2 emissions and hydrothermal unrest following the 2015 earthquake in Nepal. Nature communications 9(1): 1–10. DOI: 10.1038/s41467-018-05138-z.
35. Métivier, L., de Viron, O., et al. (2009). Evidence of earthquake triggering by the solid earth tides. Earth and Planetary Science Letters 278(3-4): 370-375. DOI: 10.1016/j.epsl.2008.12.024.
36. Lix C., Zuddas P., Guichet X., et al. (2020). Role of CO_2 in low to medium enthalpy geothermal systems in the Central Betic Cordillera (Spain). Science of the Total Envrionment 705: 13652. DOI: 10.1016/j.scitotenv.2019.135652.

FUNDING AND ACKNOWLEDGMENTS

This research was partially found by Sorbonne University and Muséun National d' Histoire Naturelle joint program Emergence n°202010261122600011JBB. The funders had no role in study design, data collection and analysis, decision to publish, or preparation of the manuscript. We thank Drs J.L. Le Moeul and G. Chiodini for helpful discussions during the writing time of the work, R. Silver for English editing as well two anonymous reviewers for useful comments that improved the clarity of the manuscript.

AUTHOR CONTRIBUTIONS

P. Z. and F. L. conceived and performed this manuscript.

DECLARATION OF INTERESTS

The authors declare no competing interests.

DATA AND CODE AVAILABILITY

All data and code are available from the corresponding author upon reasonable request.